JOURNAL OF SOLID STATE CHEMISTRY 9, 103–119 (1974)

Multiple Beam Direct Lattice Imaging of the Hexagonal Ferrites*

J. VAN LANDUYT AND S. AMELINCKX†

Fakulteit der Wetenschappen, Rijksuniversitair Centrum Antwerpen, Middelheimlaan, 1, Antwerpen, Belgium

AND

J. A. KOHN AND D. W. ECKART

US Army Electronics Technology and Devices Laboratory (ECOM), Fort Monmouth, New Jersey 07703

Received April 13, 1973

A wide variety of stacking sequences has been studied by means of transmission electron microscopy in the hexagonal ferrites of the type M_nY_m. On comparing, for a given specimen, the stacking sequences as deduced from X-ray diffraction with the image obtained in the electron microscope it was possible to establish simple "imaging codes" applicable under different diffraction conditions.

The observations are in agreement with the structural features derived from X-ray diffraction. A number of known stacking sequences has been confirmed and a number of new ones has been found as well.

The structural features of the hexagonal ferrites are reinterpreted in terms of repeated, polysynthetic twinning, the twin plane being localized in the center of the M block. Such an interpretation is suggested by the electron microscopic observations. Twinning is accompanied by a change in composition: it is therefore called *nonconservative twinning*. It is in fact analogous to crystallographic shear in accommodating deviations from simple stoichiometry. The generation of regular twinning sequences is tentatively interpreted in terms of the growth process.

1. Introduction

The hexagonal ferrites form a most remarkable group of complex oxides, exhibiting a large number of different stacking sequences of the same layer-like building units; these give rise to hexagonal unit cells with c parameters ranging up to 1600 Å. Several families of compounds having a close structural relationship can be formed. One particularly prolific family is the so-called M_2Y_n series, which contains two kinds of blocks, M and Y, in varying proportions and permutations. We shall be concerned mainly with observations pertaining to this series of compounds.

Since the thicknesses of M and Y blocks are different, it should be possible to make the stacking sequences directly visible in the electron microscope by resolving the layer planes. The relatively heavy Ba ions are localized in c layers, i.e., planes perpendicular to the c axis, therefore the most intensely diffracting material is concentrated in such planes, and conditions should be particularly favorable for direct imaging of these layers. This technique should also make it easy to determine very complicated sequences, with very large unit cells, as well as irregular sequences.

2. The Structure of the Hexagonal Ferrites

Only the structural features required for a proper understanding of the electron microscopic observations will be described here. In particular, we shall focus attention on the oxygen–barium framework. The Me^{II} and Fe ions are located in interstices determined by this framework.

* Work performed under the auspices of the Association RUCA-SCK.

† Also at S.C.K.-C.E.N. Mol-Donk, Belgium.

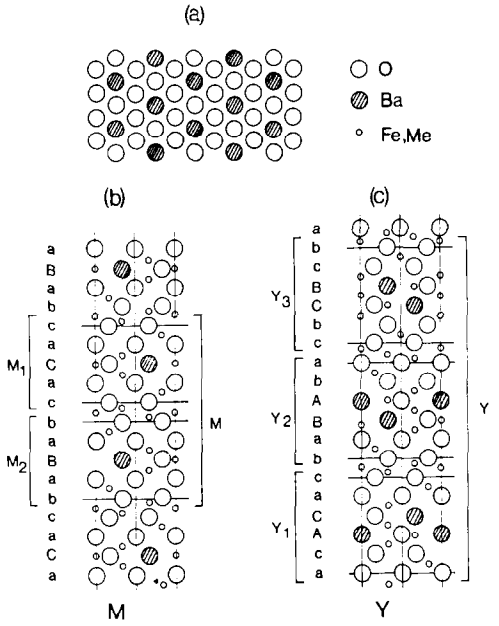

FIG. 1. (a) The structure of the close packed Ba–O layers; (b) structure of the pure M compound; (c) structure of the pure Y compound. The large open circles represent oxygen, the large cross-hatched circles represent barium ions. The small circles represent iron and zinc ions (after J. Smit and H. P. J. Wijn, "Ferrites", Wiley, New York (1959)).

The layer sequences in the oxygen–barium framework can be represented by means of the stacking symbols for close-packed layers. We shall use lower case letters, a, b, c, to represent close-packed oxygen layers, and capital letters, A, B, C, will be used to represent mixed barium–oxygen (Ba–O) layers; the latter contain one barium ion for every three oxygen ions, according to the pattern of Fig. 1a.

2.1. *The M Structure*

The pure M structure, which has the composition $BaFe_{12}O_{19}$, is hexagonal (Fig. 1b). It can be represented by means of the stacking symbol

23.2 Å

...caCacbaBabcaCac...

M_1 M_2 M_1

It consists, in fact, of two M blocks, each with a thickness of 11.6 Å, which are rotated with respect to each other by an angle of 180° about the *c* axis. This can easily be deduced from the stacking symbol; changing b into c but leaving the a-positions invariant, as is the relationship across the boundary of M_1 and M_2, is equivalent to a rotation of 180° about the *c* axis. An alternative description is that the barium-containing layer is a mirror plane for the structure. The subdivision into blocks is clearly arbitrary, however, the choice indicated above emphasizes the symmetry within a single block; it also indicates that in a given M block only *two* positions, in projection, are used for oxygen and barium. This allows the notation to be simplified even further; for the structure shown in Fig. 1b it can be written as C(a)B(a)C(a). One can consider the following M structures:

$$\ldots A(c)B(c)\ldots;\ \ldots B(a)C(a)\ldots;$$
$$\ldots C(b)A(b)\ldots$$

These structures differ only by a parallel displacement, since their stacking symbols can be transformed into each other by means of a cyclic permutation of the letters.

The symbols B(c)A(c), C(a)B(a), and A(b)C(b) represent the same structures as A(c)B(c), B(a)C(a), and C(b)A(b), respectively, since the structure contains a mirror plane normal to the stacking direction. Within each pair of constituent blocks, the small letter is always the same and differs from the two capital letters. The contact between two successive barium-containing layers is made by means of two "lamellae" in the cubic arrangement, such as

...acba...

2.2. *The Y Structure*

The Y structure is rhombohedral; three identical, translated, primitive Y blocks are required for repetition in the *c* direction (Fig. 1c). The *c* parameter is 43.56 Å; the thickness of one Y block is therefore 14.52 Å. The chemical composition of one primitive cell consisting of a single Y block is $Ba_2Me^{II}Fe_{12}O_{22}$ (in our case Me = Zn).

The *c*-layer stacking sequence can be represented by the stacking symbol

43.56 Å

...acACacbaBAbacbCBcb...

Y_1 Y_2 Y_3

Here again the subdivision into blocks is, of course, arbitrary. However, the chosen representation emphasizes the fact that in each Y

block only *two* positions are used, in projection, for oxygen and barium, as in the M blocks. The main difference is that now *two* Ba–O layers are present in each block. As far as the oxygen–barium framework is concerned, the three Y blocks, Y_1, Y_2 and Y_3, differ only by a parallel translation, since their stacking symbols are related by cyclic permutations of the letters.

The stacking rule is the same as that for M blocks, i.e., the contact between successive barium-containing layers is made by means of two "lamellae" in the cubic arrangement:

$$\ldots \underbrace{a\,\overline{c\,b\,a}}\ldots$$

The notation can in fact be condensed even further by noting simply $Y_1 \equiv [AC]$, $Y_2 \equiv [BA]$ and $Y_3 \equiv [CB]$. It is clear that the mirror images of these three blocks, i.e.,

$$Y_1^* \equiv [CA] \quad Y_2^* \equiv [AB] \quad Y_3^* \equiv [BC],$$

differs patially from their counterparts since the Y blocks have no mirror plane, but they are equally probable. The Y structure itself has *no* mirror plane either, therefore $Y_1Y_2Y_3$ and $Y_3^*Y_2^*Y_1^*$ are spatially different structures; they are twin related.

2.3. *The Z Structure*

The Z structure can be described by means of the following layer sequence:

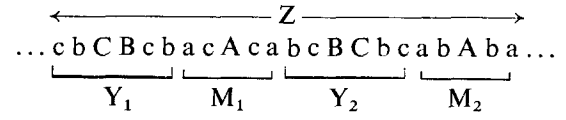

It consists, in fact, of a regular alternation of M and Y blocks and can be represented by the symbol MYMY.... It should be noted that the same layer stacking principle still applies; the junction between barium-containing layers in adjacent blocks is made by means of two overlapping triplets of layers in the cubic arrangement. The shorthand notation for the Z structure is

$$\ldots [CB]\,A(c)\quad [BC]\,A(b)\ldots$$

The Y blocks on either side of a given M block are mirror related, i.e., the mirror plane of the M block is also a mirror plane for the Z structure.

3. Planar Faults in M and Y Structures

We shall only consider faults introduced by deviations from the ideal composition. Excess barium can clearly be incorporated in the M structure by the introduction of Y blocks, since these contain two layers of Ba–O compared with one in the M block. Conversely, a deficiency of barium can be incorporated into the Y structure by the introduction of M blocks. For large deviations from the M or Y composition, regular sequences containing M and Y blocks result. We shall discuss these three cases separately.

3.1. *Faults in the M Structure*

The introduction of one Y block into the M structure results in a sequence such as

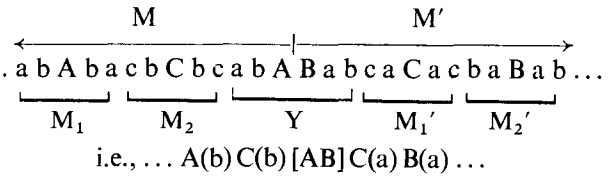

Cyclic permutations of the symbols for M_1' and M_2' reduce them to those for M_1 and M_2, respectively. This demonstrates that the two M structures on either side of the Y block are related by a *pure translation* which has a *component parallel* and also a *component perpendicular* to the *c* plane, since there is one more layer in the Y block than in the M block. The interface, therefore, is a nonconservative displacement fault, i.e., a *crystallographic shear plane*. Such faults, if inclined to the electron beam, will be imaged in the electron microscope by means of α-fringes (*1*). The introduction of a unit containing more than one Y block will, of course, change the displacement vector; the result will again be equivalent to a pure displacement fault, except when the number of Y blocks is a multiple of three, in which case the displacement vector

would have no component normal to the c axis.

3.2. *Faults in the Y Structure*

The introduction of one M block into the Y structure results in a layer sequence given by the symbol

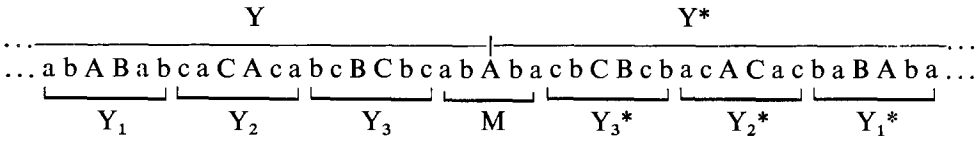

where Y* is the mirror structure of Y. A twin has been generated, with the mirror plane of the M block as a coherent twin plane; at the same time some barium deficiency has been incorporated into the structure. One can, in fact, ignore the M layer and consider the resulting structure as a twin in the pure Y configuration, the twinning being accompanied by the removal of one Ba–O layer. We shall call such an interface a *non-conservative* twin plane.

Such a planar fault, if inclined to the electron beam, will be imaged by means of wedge fringes if only one part of the twin is in a reflection position. The two parts of the twin will exhibit a different intensity for certain reflections other than those of the [000l] row. The introduction of a second M block at another point reinstates the original structure, the two equivalent parts being separated by a twin lamella.

The thickness of this twin lamella will determine whether or not the two parts on either side of it are shifted with respect to each other. The following different cases are possible:

displacement of the two Y structures along a vector parallel to the c axis; (2) and (3), on the other hand, lead to displacement vectors with an additional component normal to the c axis.

In all cases, two successive M blocks of the sequence, even though separated by an arbitrary number of Y blocks, have the same relative orientations as in the pure M structure, provided that the junctions between M and Y blocks consist of two triplets in the cubic arrangement. This means that successive M blocks differ in orientation by a c axis rotation of 180°, a factor of importance with respect to contrast behavior in the electron microscope.

3.3. *Mixed-Layer Structures*

In structures of the type MY_nMY_m, the sum $m+n$ gives the composition of the resulting crystal directly. If $m+n=m'+n'$ with $m \neq n$, MY_nMY_m and $MY_{n'}MY_{m'}$ have the same chemical composition but different structures; they are called *mixed-layer polytypes*. Such crystals differ only in the stacking arrangement of the same layers; as a result, however, they may belong to different space groups (*2*).

More complicated sequences containing more than two isolated M layers are also observed. Since the introduction of one M layer is equivalent to twinning, it is clear that, in any case, the repeat unit in the c direction should contain an even number of M blocks.

...[AB][CA][BC]A(b)C(b)[AB][CA][BC]... (1)

...[AB][CA][BC]A(b)[CB]A(c)[BC][AB][CA] (2)

...[AB][CA][BC]A(b)[CB][AC]B(a)[CA][BC][AB]... (3)

...[AB][CA][BC]A(b)[CB][AC][BA]C(b)[AB][CA][BC]... (4)

In (1), the two M blocks are adjacent, whereas in (2), (3) and (4) they are separated by a twin lamella which is, respectively, one, two or three Y-blocks thick. It can be seen from the stacking symbols that if the twin band has a thickness of $(3n+r)$ Y blocks, with $r=0$, 1 or 2, the two Y structures on either side of the twin are shifted over r steps, i.e., one needs r cyclic permutations of the letter sequence ABC to achieve coincidence. Cases (1) and (4), therefore, lead to a relative

Let the general block symbol be

$$MY_{r_1}MY_{r_2}MY_{r_3}\ldots MY_{r_{2n-1}}MY_{r_{2n}}. \quad (5)$$

We can then consider the number,

$$\Delta = \sum r_{\text{odd}} - \sum r_{\text{even}},$$

given by the sum of the r values with an odd index minus the sum of the r values with an even index.

If $\Delta = 0 \pmod 3$, the resulting structure is hexagonal, and Eq. (5) is the block symbol for the repeat unit along the c axis. On the other hand, if $\Delta = \pm 1 \pmod 3$, then the resulting structure is rhombohedral, and the repeat distance in the c direction contains three times the number (N) of anion layers given by Eq. (5) where

$$N = 10n + 6 \sum_{j=1}^{2n} r_j.$$

Short symbols for these different hexagonal ferrite structures were introduced earlier (*3*); they are $N\mathrm{H}_a$ or $3N\mathrm{R}_b$, where subscripts a, b,... are used to denote the different polytypes within a given group. A more descriptive notation has also been used (*4*, *5*), which indicates the number of Y blocks in each band, e.g.,

$$3N\mathrm{R}_{r_1 r_2 \ldots r_{2n}},$$

or

$$N\mathrm{H}_{r_1 r_2 \ldots r_{2n}}.$$

As we have seen above, the introduction of one M block is equivalent to twinning; the introduction of a second M block restores the original sequence. Successive Y bands will therefore be in twin orientation, whereas alternating Y bands will be in the same orientation.

It is possible to reveal these twin bands in the electron microscope as bands of different intensity; this is discussed below.

4. Experimental Methods

4.1. Specimen Preparation

The crystals, hexagonal plates parallel to the basal (c) plane, were grown from $NaFeO_2$ and BaO/B_2O_3 fluxes (*6*, *7*). All crystals were characterized by means of Weissenberg X-ray diffraction patterns. Some of the specimens contained only one layer sequence; others contained several layer sequences as detected by X-ray diffraction. Most of the crystals examined in the electron microscope were characterized by Weissenberg diffractometry as being of the M_2Y_n type.

Since the main interest is in the study of block sequences, it is necessary to have very thin specimens with the specimen plane perpendicular to the c (basal) plane, in order to resolve individual blocks.

Some specimens were first prepared by sawing c platelets perpendicular to the basal plane and then thinning them by ion bombardment under grazing incidence. This procedure was not very successful because of the small size of the crystals and the rather pronounced basal cleavage.

Most of the specimens actually examined were finally obtained by grinding the crystals and dispersing the fragments in alcohol on thin, perforated, carbon films.

Fortunately, apart from the basal cleavage, a rather pronounced prismatic cleavage is present as well. By chance, we were able to find some very thin flakes that had cleaved along such a prismatic plane, with the right orientation and partly covering a hole in the supporting film; these proved to be the best specimens for our purpose.

4.2. Electron Microscope Observation Techniques

Utilizing the goniometer stage, specimens are brought into an orientation such that the incident electron beam is exactly parallel to the layer (c) planes. This can be achieved by using the electron microscope in the diffraction mode and orienting the crystal such that a systematic row of closely spaced diffraction spots of the type $000l$ is visible over its whole length.

Dark-field images produce the best contrast. The dark-field image is made by beam deflection, without changing the specimen orientation. The aperture is chosen so as to admit at least three main spots, i.e., corresponding to the block spacing (11–12 Å; 14–15 Å) and inevitably several superlattice spots. The best contrast is obtained by slight underfocusing.

Lattice fringes have optimum visibility in the extinction contours corresponding to the selected spots. The best images are formed in those areas where the bright extinction contours extend into the thinnest part of the specimen, i.e., come close to the crystal edge. To obtain maximum resolution, several images, differing slightly in focus (so-called "through focus series"), are often made. In order to obtain comparable images for the different mixed-layer polytypes, the same set of main spots was always selected with the same aperture.

Figure 2a gives an example of the type of line image obtained in this manner; it contains two different spacings. The inset shows the set of diffraction spots selected.

In a number of cases the crystals were oriented such that a large area of a reciprocal lattice plane containing several parallel, densely populated rows of spots became visible in the diffraction pattern (Fig. 3). Dark-field images were then made using rows of spots not necessarily of the

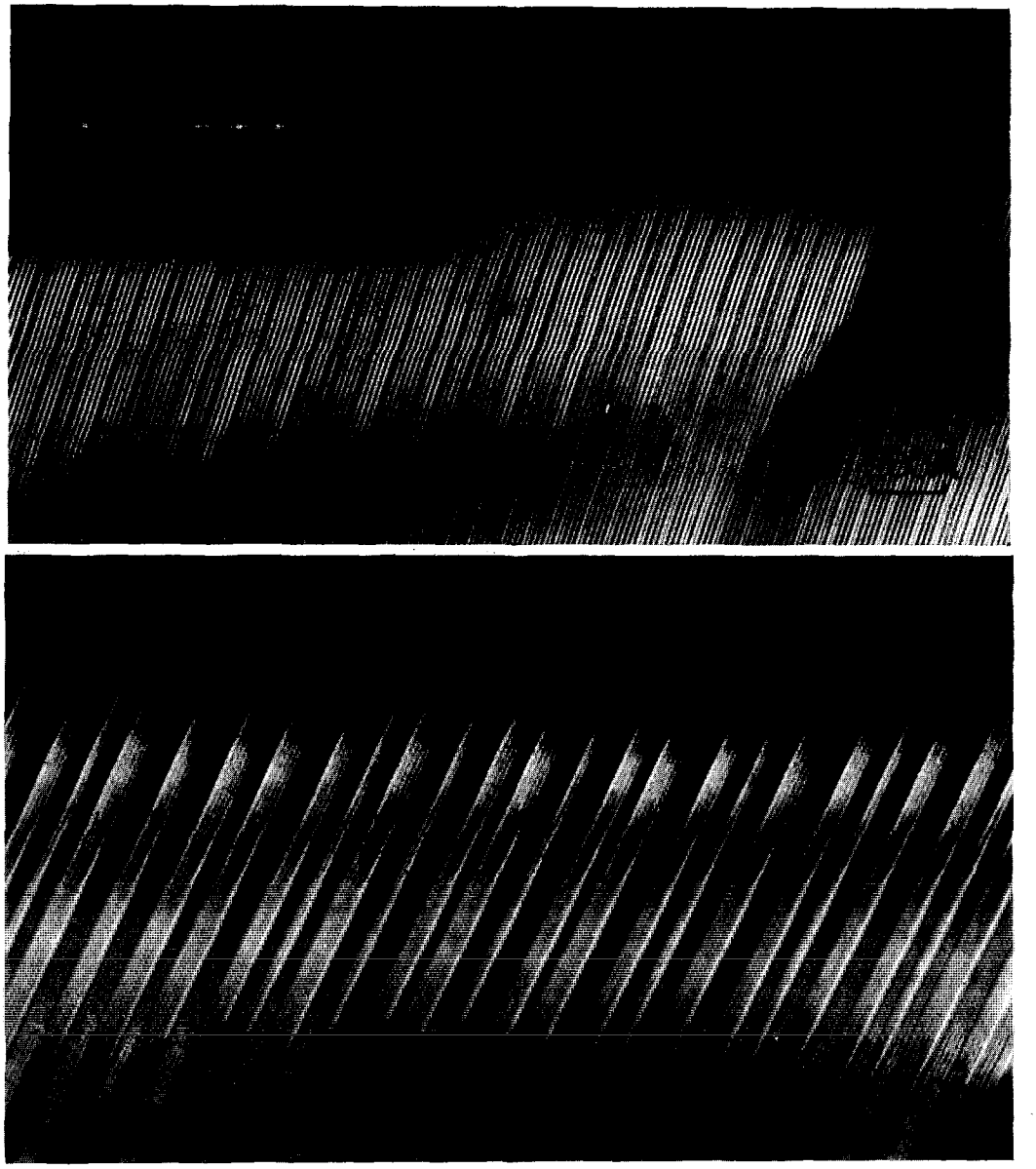

FIG. 2. (a) Typical dark-field line image obtained by selecting the indicated diffraction spots of the [000*l*] row. (b) Corresponding dark-field image taken in off-central row spots. Successive Y bands exhibit a different shade.

000*l* type. In this way one is most apt to find contrast differences between successive Y bands. Lattice fringes are usually visible within the Y bands as well (Fig. 2b).

4.3. Width Measurements

Since the M blocks appear only as isolated layers in the sequence, it is difficult to perform precise width measurements; the following methods, however, permit a somewhat higher precision.

One measures the width t_i of a band containing a number m_i of M blocks and a number y_i of Y blocks. Denoting the width of an M block and of a Y block, respectively, as w_M and w_Y, one obtains a number of equations for different sequences containing M and Y blocks in varying proportions:

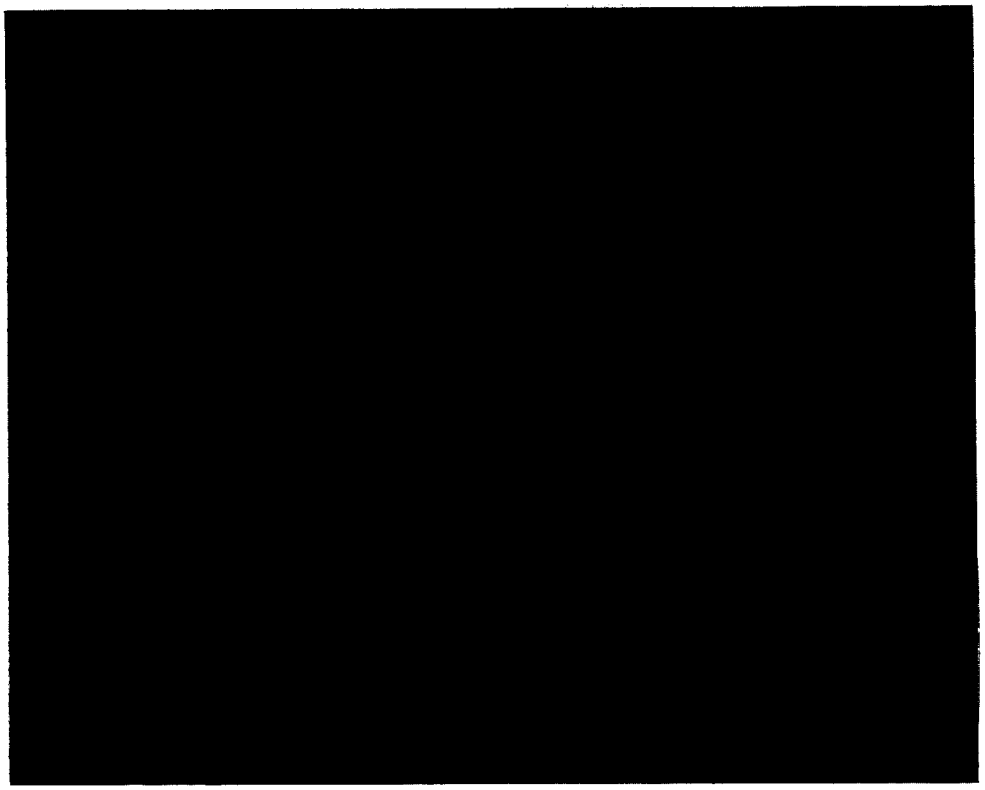

FIG. 3. Typical diffraction pattern; the circles indicate the position of the aperture when selecting typical groups of spots used for making dark-field images (1) group of spots in the [000*l*] row (2) off-central row group of spots.

$$t_i = m_i w_M + y_i w_Y .$$

The equations can be solved for the best values of w_M and w_Y by the method of least squares.

Since we are actually more interested in the *ratio* of block widths rather than in *absolute* values, we measured the number of blocks of each kind contained within an equivalent distance Δ over different regions of the same photograph; such regions were selected to maximize differences in the relative concentrations of M and Y blocks. One then finds:

$$\Delta = m_i w_M + y_i w_Y = m_j w_M + y_j w_Y ,$$

and thence:

$$\frac{w_Y}{w_M} = \frac{m_i - m_j}{y_j - y_i} .$$

A large number of such measurements leads to a value of

$$(w_Y/w_M) \text{ measured} = 1.26 \pm 0.07,$$

which is in good agreement with our assumption that the narrow strips image M blocks and the wider strips Y blocks, since

$$(w_Y : w_M)_{\text{X-ray}} = 1.251.$$

5. Experimental Results

5.1. The Imaging Code

Observations noted above strongly suggest that the two observed spacings in the well-resolved line patterns correspond to the different thicknesses of M and Y blocks.

If this is true, it is a simple matter to deduce the layer sequences directly from the micrographs, associating a pair of closely spaced lines with an M block and a pair of more widely spaced lines with a Y block. There are a number of arguments supporting this very simple "imaging code":

i. The closely spaced pairs of lines, which sometimes appear as a single, wide, diffuse dark line, always occur isolated, which is the behavior already noted for M blocks in crystals at the Y-rich end of the M–Y pseudo-binary system.

ii. The layer sequences deduced from electron micrographs using this "code" correspond, in general, with the most frequently occurring layer sequences deduced from respective Weissenberg patterns. In most crystals, layer sequences *not* detected by the Weissenberg method were found in the micrographs as well, a fact which can be explained by assuming that they were present in only a small volume of the crystal.

iii. The most direct verification undoubtedly consists in measuring the widths of the two kinds of strips on the micrograph and comparing these with the known thicknesses of M and Y blocks. Unfortunately, since the M blocks appear only as isolated layers in the sequences, such a measurement is difficult to perform with any precision. However, since the ratio of the number of M blocks to the number of Y blocks varies in different sequences, one can use the method described in Sect. 4.3 in order to achieve a higher precision; these measurements again confirm the simple rule.

iv. The imaging code is consistent with the dark-field images taken in off-central row spots. According to the structural considerations noted in Sect. 3, successive bands are in twin relationship, and the transition region between two Y blocks can be described as an M block. The exact correspondence between the *line image* and the *band image* of Fig. 4 proves that the contact region is indeed imaged in the line pattern as two lines with a spacing smaller than that for a Y block. The contrast difference between successive Y bands is further consistent with the fact that these bands are in twin orientation; this, in turn, proves that they are indeed Y bands, because the *c* plane can be a twin plane for the Y structure but not for the M structure (the M structure has a mirror plane parallel to the *c* plane).

That the *c* plane is the twin plane is also consistent with the absence of band contrast when only the [000*l*] systematic row of reflections is operating.

All these arguments prove beyond any reasonable doubt that the simple imaging code is correct.

5.2. Regular Stacking Sequences

Using the type of contrast for which the imaging code has been established, line images were recorded for some 14 different simple sequences. Enlarged typical areas are assembled

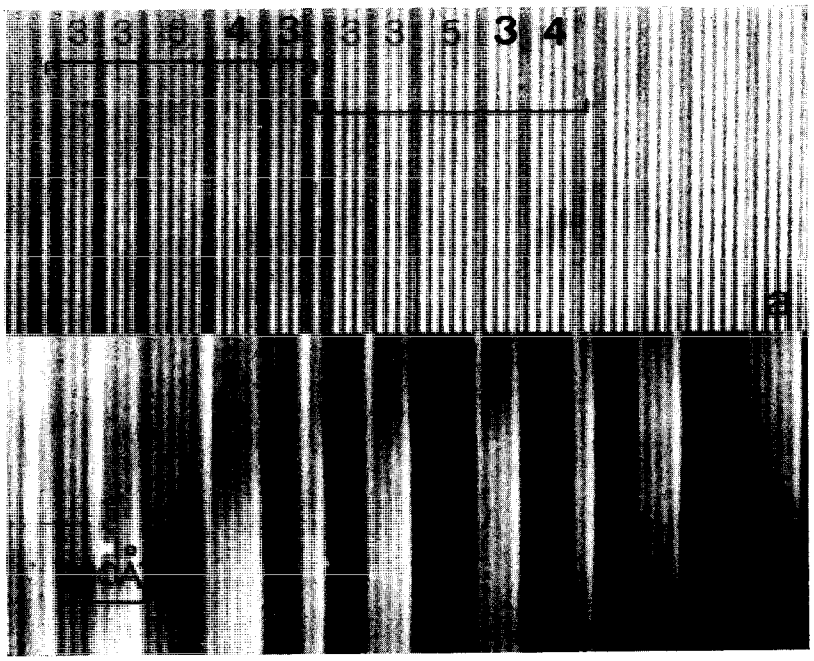

FIG. 4. Correspondence between the line image and the band image of the same sequence. Successive M blocks are imaged alternatively as bright and dark lines. The sequence is part of a larger regular sequence; the part shown contains a sequential fault.

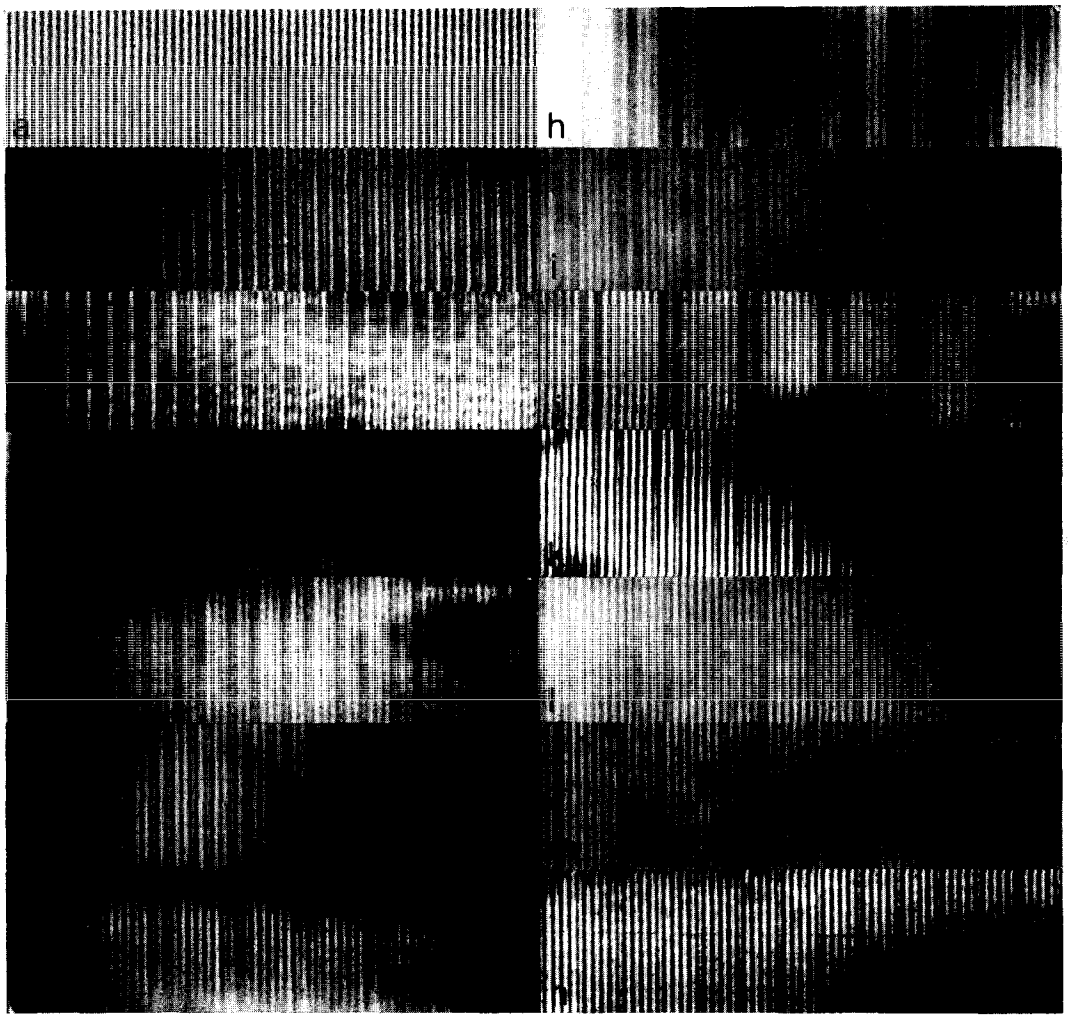

FIG. 5. A number of regular sequences. The characteristics of the different sequences are summarized in Table I.

TABLE I

M:Y	Stacking sequence	Fig.
1:∞	Y	5(a)
2:1	MMY	5(c)
2:2	MYMY	5(b)
2:3	$MYMY_2$	5(f)
2:4	$MYMY_3$	5(h)
2:5	MY_2MY_3	5(e)
2:6	$MYMY_5$	5(i)
	MY_2MY_4	5(k)
	MY_3MY_3	5(d)
2:7	$MYMY_6$	5(g)
2:8	$MYMY_7$	5(j)
	MY_4MY_4	5(n)
2:10	MY_3MY_7	5(l)
2:11	MY_4MY_7	5(m)

in Fig. 5. Table I gives a survey of the observed structures and provides the block notations for the different sequences as well. Most of these structures were known previously from X-ray diffraction, but one (My_3My_7) is established here for the first time.

Of the specimens examined, except for the case of MMY, the M block always occurred in an isolated mode, even in irregular sequences. This supports a tendency already known from X-ray diffraction; it is explained below.

The advantages of direct imaging electron microscopy, compared to X-ray diffraction, are most evident for long and complicated sequences. Three such examples are reproduced in Figs. 6 and 7, and their stacking sequences are given in Table II.

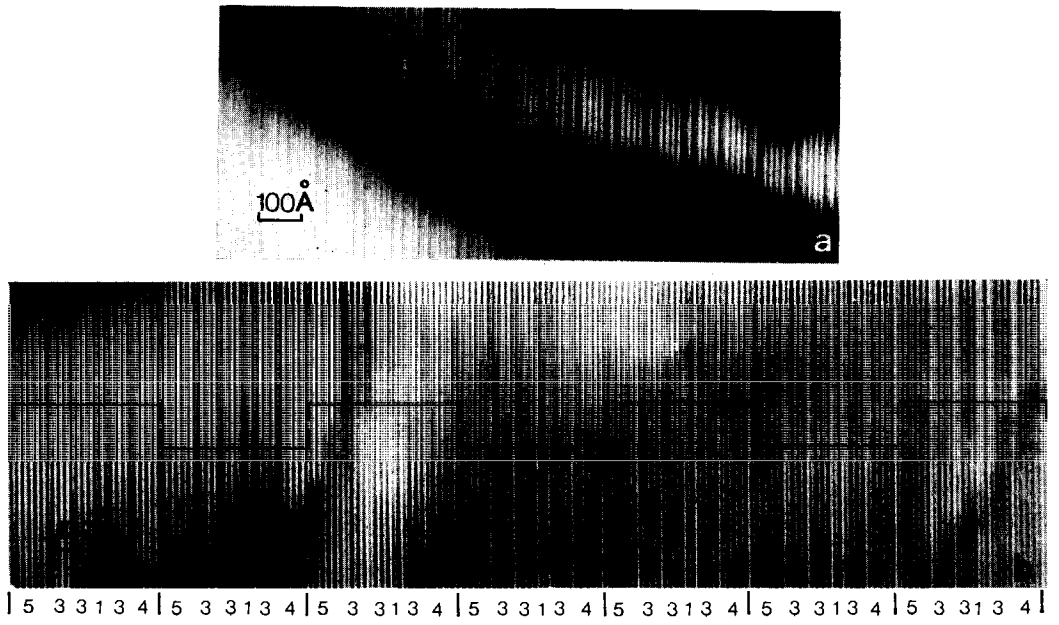

FIG. 6. (a) Complicated stacking sequence. The photograph shows only a small number of stacking periods out of a much larger sequence. (b) Complicated stacking sequence. The characteristics of these sequences are summarized in Table II.

TABLE II

M:Y	Stacking sequence	Short notation	Fig.
6:19	$MYMY_3MY_4MY_5MY_3MY_3$	$144H_{1\text{-}3\text{-}4\text{-}5\text{-}3\text{-}3}$	6b
8:18	$MYMY_4MYMY_4MYMY_4MYMY_2$	$444R_{1\text{-}4\text{-}1\text{-}4\text{-}1\text{-}4\text{-}1\text{-}2}$	6a
6:21	$MY_3MY_3MY_3MY_4MY_4MY_4$	$468R_{3\text{-}3\text{-}3\text{-}4\text{-}4\text{-}4}$	7

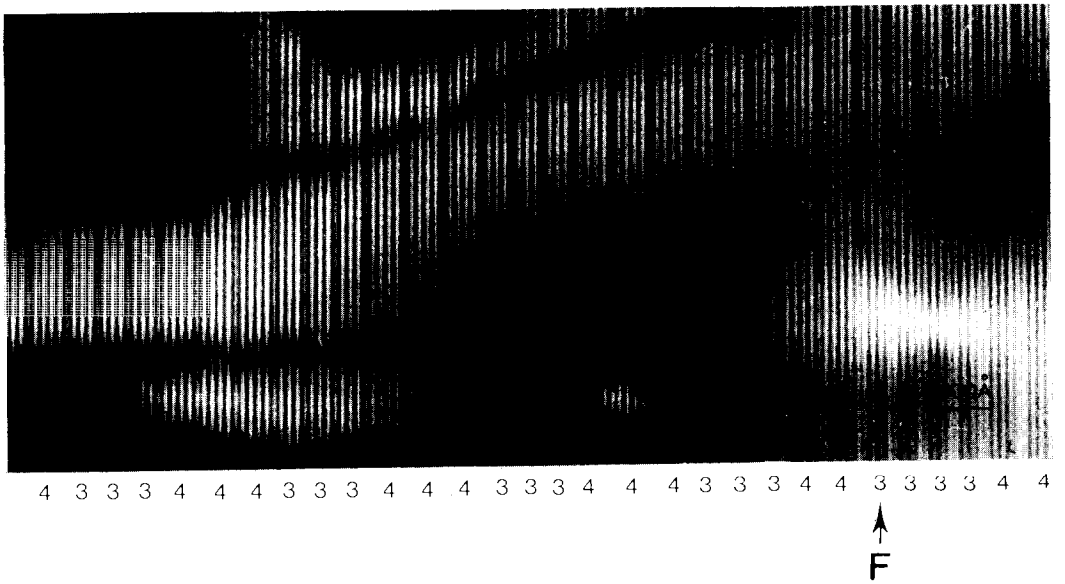

FIG. 7. Complicated sequence containing one stacking fault indicated in F. The characteristics of the sequence are summarized in Table II.

The first of these sequences has an M:Y ratio of 6:19, and the resulting crystal is hexagonal with a unit cell containing 144 anion layers; the stacking symbol described in Refs. (*4*, *5*) can be written as $144H_{1\text{-}3\text{-}4\text{-}5\text{-}3\text{-}3}$. The one to one correspondence between the line pattern (central line dark-field image) and the corresponding band pattern (off-central line dark-field image) for this structure is shown in Fig. 4; it proves, as is shown below (Sect. 6), that the structure can also be described in terms of periodic polysynthetic twinning.

The second sequence has an M:Y ratio of 8:18; the resulting crystal is rhombohedral, containing $148 \times 3 = 444$ anion layers in the unit cell. Using the short notation, the stacking symbol is $444R_{1\text{-}4\text{-}1\text{-}4\text{-}1\text{-}4\text{-}1\text{-}2}$. This structure can be considered a periodically faulted variant of the simpler $MYMY_4$ structure. The third sequence has an M:Y ratio of 6:21 and the corresponding stacking symbol is $468R_{3\text{-}3\text{-}3\text{-}4\text{-}4\text{-}4}$. The part of the sequence shown in Fig. 7 contains one fault at F.

It is quite an interesting problem to understand how regular sequences of such great lengths can be generated.

5.3. Faulted and Irregular Sequences

Isolated faults, perturbing the regularity of the sequences, occur rather frequently. Some examples of faults in simple structures are shown in Fig. 8a, as revealed by their line patterns. Widely separated, isolated faults in regular sequences can also be revealed by means of stacking fault fringes; an example of this is reproduced in Fig. 8b, which corresponds with the line pattern of Fig. 8a. As a consequence of the large extinction distance, no well-defined fringes are visible.

In Fig. 4, the regular sequence $MYMY_3MY_4$-$MY_5MY_3MY_3$ contains one sequence of layers $MYMY_4MY_3MY_5MY_3MY_3$ with the same length as the original sequence but with one of the M blocks at a different location. This changes neither the stoichiometry nor the unit cell size; we propose to call such a fault a *polytypic fault* or, since it must always occur in pairs, a *sequential fault*.

For crystals with a composition close to pure Y, there seems to be a rather pronounced tendency to form, within a matrix of Y, sequences of the type Y...YYMYMY...Y, i.e., two M blocks separated by a single Y block. This

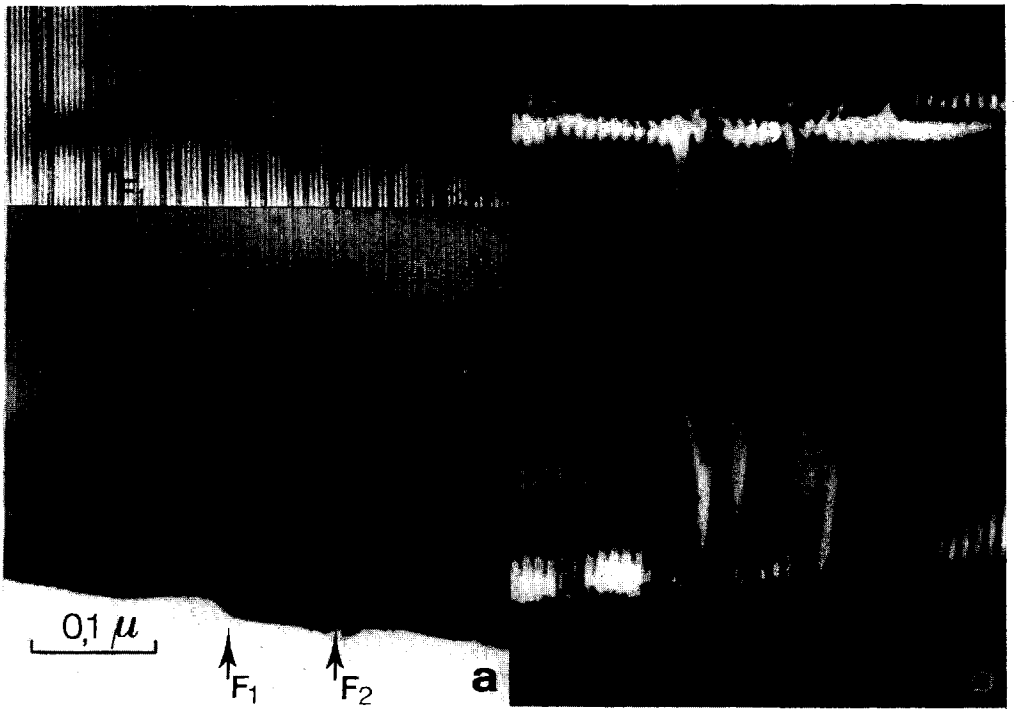

FIG. 8. (a) Two faults in a regular sequence of the type MY_2MY_4. In F_1 one band Y_4 is replaced by a band Y_2; in F_2 *two* adjacent M layers are present, which is highly exceptional. (b) Fringe contrast at the two stacking faults in (a).

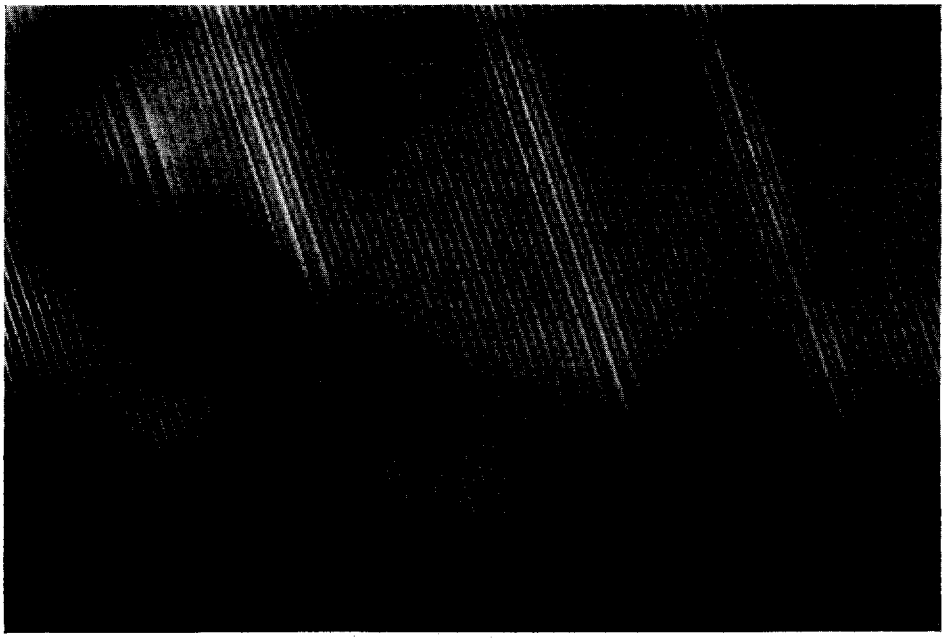

FIG. 9. Sequence of Y blocks interrupted by a number of faults Y...YMYMY...Y which can be considered as twins of minimum width.

configuration is equivalent to a twin of minimum width; several examples are visible in Fig. 9.

Irregular sequences occur rather frequently as well; they range from completely disordered (Fig. 10a) to regular sequences containing isolated faults (Fig. 10b). An irregular sequence, corresponding with an average M:Y ratio of 2:5, is shown in Fig. 10a. In spite of the quite irregular character of the sequence, the tendency for no adjacent M blocks to be present is still valid. This is easy to understand, since the M block is, in fact, an alternative description of a twin plane. The statement that no two M blocks are adjacent is equivalent to saying that the twin lamellae have a minimum thickness of 11 anion layers.

6. Contrast Effects

Dark-field images taken with spots of the [000*l*] systematic row, and with no other rows of spots excited, produce the type of line contrast which lends itself to the easiest interpretation. The sequences can then be deduced from the spacings between lines (see Sect. 5).

A different imaging code is applicable for slightly different orientations. Figure 11a and b shows the same sequences; in Fig. 11a the usual contrast conditions, discussed above, prevail; in Fig. 11b the orientation is slightly different, although spots of the [000*l*] row are still the only ones excited. The sequence can now be deduced by associating the lines themselves with the blocks: a heavy black line (on a positive print) has to be associated with a Y block and a much weaker black line with an M block.

Additional information can be extracted from dark-field images using 000*l* reflections, with the simultaneous excitation of spots from other reciprocal lattice rows. Successive Y bands as well as successive M blocks, now exhibit somewhat different contrast behavior. These effects are even more pronounced when dark-field images are made in reflections belonging to non-central rows of spots with $h-k \neq 0 \pmod 3$. Under these conditions, successive Y bands show up with a strikingly different intensity, consistent with our description in terms of twins.

Figure 4 shows an example of a dark-field line pattern (in 000*l* reflections) and the corresponding DF patterns taken in spots of a parallel non-central row. The alternating bright and dark regions clearly image Y bands. The M blocks do not produce an easily identifiable image in the band picture (Fig. 4b). Within the Y bands, one can still identify individual Y blocks. It is clear that with the Y bands there are only two types of

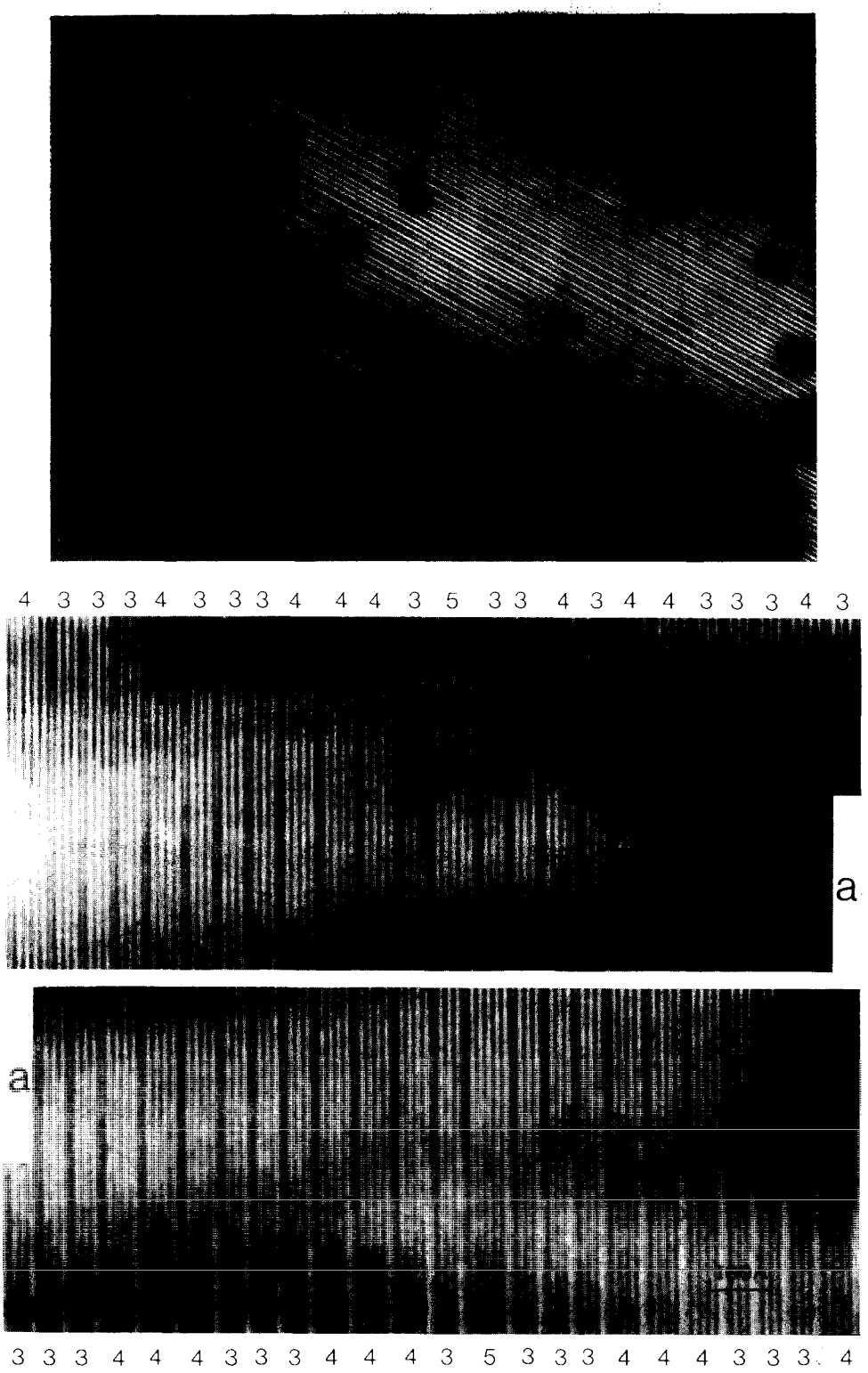

FIG. 10. (a) Highly irregular sequence; (b) faults in a complicated sequence $MY_3MY_3MY_3MY_4MY_4MY_4$ of which a regular part is shown in Fig. 7. (The two parts of photograph (b) should be joined along the strips labeled (a).)

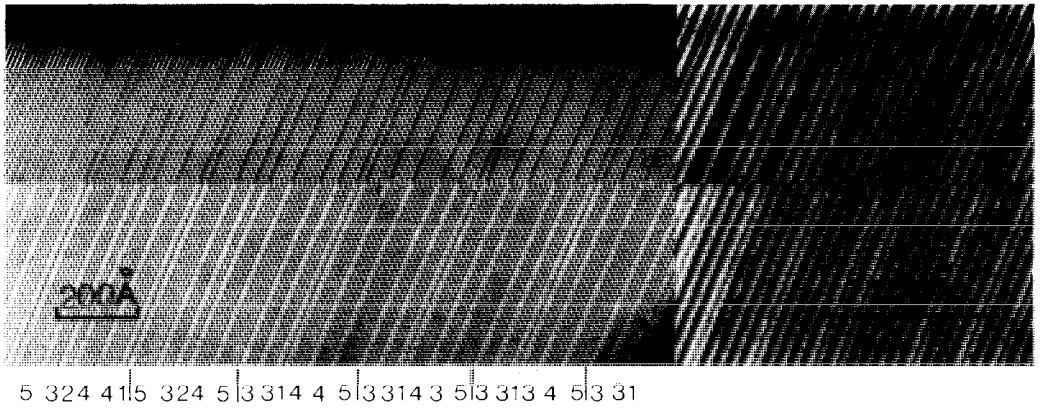

FIG. 11. The same sequence shown under two different diffraction conditions. (a) The lines can be considered as the block boundaries; the M blocks are narrower than the Y blocks. (b) The lines mark the blocks; Y blocks are marked by heavier lines than M blocks. Note the exact correspondence between the two imaging codes.

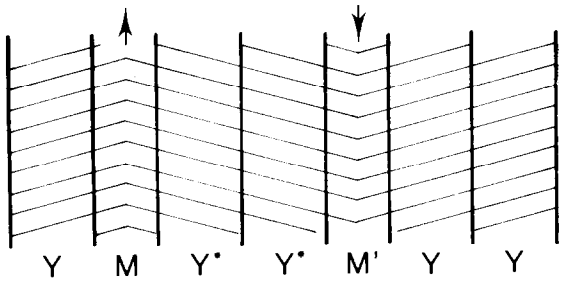

FIG. 12. Schematic representation of the twin structure of the different sequences. The twin plane is associated with the M block.

background intensity observed, suggesting that there are only two differently oriented Y bands. This contrast behavior is completely consistent with our description of these structures in terms of periodic twinning (compare schematic in Fig. 12).

Figure 4b shows another remarkable contrast feature. The position of the M block along the contact plane between successive Y bands is marked alternatively by a bright and a dark line. The character of these lines reverses on crossing an extinction contour. This contrast effect is presumably related to the fact that two successive

FIG. 13. Contrast difference between successive twin bands.

M blocks differ by a rotation of 180° about the *c* axis. For central-row spots, if in one M block the 000*l* reflections are excited, the 000*l* reflections are excited simultaneously in the next M block. In view of Friedel's law, this does not produce any contrast, unless a multiple beam situation prevails (*8*). In the latter case dark-field images made with spots from a noncentral row may produce more pronounced contrast (Fig. 13).

Figure 13 also shows that the Y blocks in one Y band have a better contrast than those in the next block.

Under certain diffraction conditions, using noncentral-row dark-field images, individual Y blocks may be observed in one set of Y bands but not in the next one.

For most line images, a somewhat lower intensity is observed for one of the two lines limiting the M block (Fig. 4a). This strongly suggests a relation to the fact that the M block contains only one layer of Ba-O versus two in the Y block. The projected electron density along this layer, therefore, is relatively smaller, probably giving rise to the slightly weaker dark line in the dark-field image. It is to be noted that in a given region, i.e., for given diffraction conditions, the weaker line is always on the same side of the M block; this side may change along the M strip with changing diffraction conditions.

7. Discussion

7.1. Stoichiometry and Nonconservative Twins

The observations described in this paper and their interpretation show that the structural complexity of the hexagonal ferrites can be simplified in a nontrivial manner by considering these structures as periodic twins; the twinning is accompanied by small changes in composition. The term *nonconservative twin* is proposed for this type of interface.

It is well known that deviations from simple stoichiometry can be accommodated into a crystal by crystallographic shear planes, sometimes also called nonconservative anti-phase boundaries (*9*). The inclusion of a Y block within an M matrix causes an excess of barium to be built into the crystal. The resulting configuration can alternatively be described as due to the introduction of a crystallographic shear plane. In this respect, the hexagonal ferrites have a behavior rather similar to other complex oxides (*10*).

In an analogous manner, a small deficiency of barium can be introduced into a Y matrix by the inclusion of an M block. We thus find that compositional changes can also be embodied as *nonconservative twins*. During the growth of these crystals from a flux of a given composition, one could imagine that quite small fluctuations in composition induce the crystal to twin or to include a crystallographic shear plane depending on whether the composition is close to Y or to M, respectively.

7.2. Growth Mechanism

In a particular growth situation, imagine that the flux contains the correct ratio of ions to produce a crystal of composition M_nY_m with $m > n$, i.e., not too far from the Y composition. In flux growth it is reasonable to assume that the growth rate will be controlled by temperature

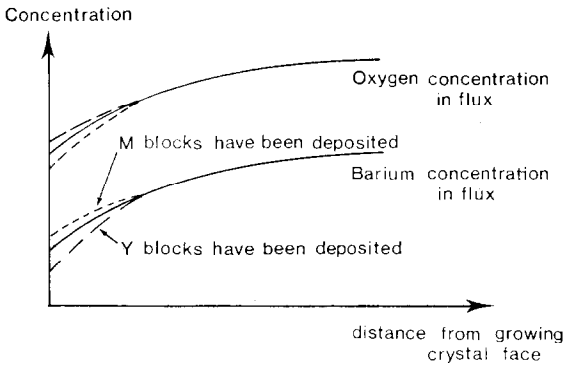

FIG. 14. Schematic representation of the variation of the concentration profile of oxygen and barium in the layer in contact with the growing crystal face.

gradients, whereas the exact chemical composition of the deposited layer may be diffusion controlled.

In order to understand the formation of successions of M and Y blocks, it is necessary to explain why at one instant during the growth process a single Ba–O layer is deposited, whereas at another instant a double Ba–O layer is formed. The following is a somewhat naïve picture which could explain this behavior. Assume for the moment that the crystal is perfect and growth proceeds by the nucleation and deposition of successive c layers. (We shall focus attention mainly on the oxygen and Ba–O layers.) The composition of the solution far from the crystal corresponds to M_nY_m. In the immediate vicinity of the growing crystal face, however, the instantaneous concentration of Ba may be slightly above or below the concentration in equilibrium with the growing crystal face, depending on whether the latest deposited layers were pure oxygen or Ba–O. If, for instance, four oxygen layers have just been deposited, the concentration of barium in immediate contact with the growing crystal has increased, and the chances for nucleation and deposition of a Ba–O layer have now become greater.

Of course, interactomic forces play an importtant role in inducing the deposition of either a single or a double Ba–O layer; such forces are apparently not a decisive factor in determining which will be deposited, however, since both M and Y blocks can appear almost at random in certain crystal regions. Energetically, there seems to be only a small difference between the two cases. It is not unreasonable, therefore, to assume that

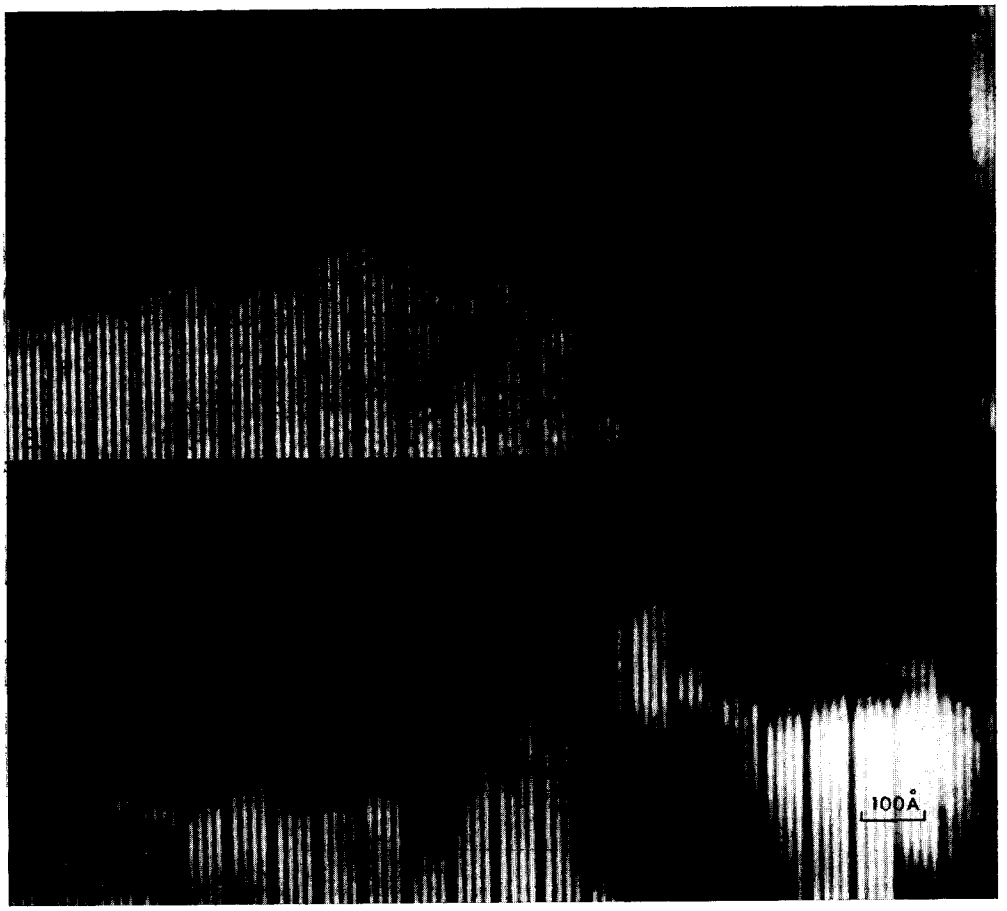

FIG. 15. The same crystal part before (a) and after (b) heating in the microscope electron beam. Note that the M blocks exhibit absorption contrast (black line) after heating.

periodic fluctuations in the composition of the layer in contact with the crystal face will cause periodic or quasi-periodic deposition of an M layer and hence periodic or somewhat random twinning.

More specifically, after a number of Y blocks have been deposited, the composition of the layer in contact with the crystal has been depleted in Ba and now a single Ba–O layer is deposited, i.e., an M block, at the same time inducing the crystal to twin.

Schematically these variations are shown in Fig. 14. The full line represents the situation after a number of Y blocks have been deposited; the Ba concentration is below average whereas oxygen is above average. The probability for depositing an M block is now large. After an M block is deposited, the situation reverts to the one represented by the broken line.

The long-range repetition of lengthy sequences strongly suggests the need to invoke another mechanism; a likely candidate is the process of spiral growth (*11*). This is a matter for separate consideration.

7.3. Local Decomposition or Melting

On careful heating in the electron microscope by means of the electron beam changes take place in the aspect of the specimen. The most remarkable feature is a change in contrast of the M-block region. After heating, this region exhibits a dark band, whereas within the Y bands no changes have taken place. Figure 15 shows the same regions of a crystal presenting the sequence MY_4MY_4, before (a) and after heating (b). This seems to prove that the M region is more sensitive to decomposition or melting than the Y bands. This behavior would be consistent with our interpretation of the M regions as twins.

References

1. R. Gevers, P. Delavignette, H. Blank, and S. Amelinckx, *Phys. Status Solidi* **4**, 383 (1964); R. Gevers, P. Delavignette, H. Blank, J. Van Landuyt, and S. Amelinckx, *Phys. Status Solidi* **5**, 595 (1964).
2. J. A. Kohn and D. W. Eckart, *Amer. Mineral.* **50**, 1371 (1965).
3. J. A. Kohn and D. W. Eckart, *Z. Kristallogr.* **119**, 454 (1964).
4. C. F. Cook, Jr., *J. Appl. Phys.* **38**, 2488 (1967).
5. J. A. Kohn, D. W. Eckart, and C. F. Cook, Jr., *Mater. Res. Bull.* **2**, 55 (1967).
6. R. O. Savage and A. Tauber, *J. Amer. Ceram. Soc.* **47**, 13 (1964).
7. R. O. Savage and A. Tauber, *Mater. Res. Bull.* **2**, 469 (1967).
8. M. Snykers, R. Serneels, P. Delavignette, R. Gevers, and S. Amelinckx, *Cryst. Lattice Defects* **3**, 99 (1972); R. Serneels, M. Snykers, P. Delavignette, R. Gevers, and S. Amelinckx, *Phys. Status Solidi*, in press.
9. M. Snykers, P. Delavignette, and S. Amelinckx, *Phys. Status Solidi (B)* **48**, K1 (1971); G. Van Tendeloo, P. Delavignette, R. Gevers, and S. Amelinckx, *Phys. Status Solidi*, in press.
10. J. S. Anderson and B. G. Hyde, *J. Phys. Chem. Solids* **28**, 1393 (1967); L. A. Bursill, B. G. Hyde, O. Terasaki and A. Watanabe, *Phil. Mag.* **20**, 347 (1969); S. Anderson and A. D. Wadsley, *Nature (London)* **5048**, 581 (1966); J. Van Landuyt and S. Amelinckx, *J. Solid State Chem.* **6**, 222 (1973).
11. C. F. Cook, Jr. and W. F. Nye, *Mater. Res. Bull.* **2**, 1 (1967); W. Tolksdorf, *J. Cryst. Growth* **18**, 57 (1973).